Structural and neurochemical correlates of individual differences in gamma frequency oscillations in human visual cortex

Siân E. Robson,[1,2] Suresh D. Muthukumarawswamy,[3] C. John Evans,[1] Alexander Shaw,[1] Jennifer Brealy,[1] Brittany Davis,[1] Grainne McNamara,[1] Gavin Perry[1] and Krish D. Singh[1]

[1]*Cardiff University Brain Research Imaging Centre (CUBRIC), School of Psychology, Cardiff University, Cardiff, UK*
[2]*Sir Peter Mansfield Magnetic Resonance Centre, School of Physics and Astronomy, University of Nottingham, Nottingham, UK*
[3]*Schools of Pharmacy and Psychology, University of Auckland, Auckland, New Zealand*

Abstract

Neuronal oscillations in the gamma frequency range play an important role in stimulus processing in the brain. The frequency of these oscillations can vary widely between participants and is strongly genetically determined, but the cause of this variability is not understood. Previous studies have reported correlations between individual differences in gamma frequency and the concentration of the inhibitory neurotransmitter, gamma-aminobutyric acid (GABA), as well as with age and primary visual cortex (V1) area and thickness. This study assessed the relationships between all of these variables in the same group of participants. There were no significant correlations between gamma frequency and GABA+ concentration, V1 area or V1 thickness, although the relationship with GABA+/Cr approached significance. Considering age as a covariate further reduced the strength of all correlations and, in an additional dataset with a larger age range, gamma frequency was strongly inversely correlated with age but not V1 thickness or area, suggesting that age modulates gamma frequency via an additional, as yet unknown, mechanism. Consistent with other recent studies, these findings do not demonstrate a clear relationship between gamma frequency and GABA+ concentration. Further investigation of additional variables and the interactions between them will be necessary in order to more accurately determine predictors of the frequency of gamma oscillations.

Key words: cortical thickness; gamma; gamma-aminobutyric acid-A; individual differences; magnetic resonance spectroscopy; magnetoencephalography; neuronal oscillations; primary visual cortex; V1.

Introduction

Neuronal oscillations are rhythmic electrophysiological signals generated by synchronous activity in large populations of neurons in the brain. These oscillations play a vital role in processing information, regulating the excitability of neurons within regions, and facilitating communication across neuronal networks in the brain. Oscillations have been measured since the 1920s using electroencephalography (EEG; Berger, 1929) and later magnetoencephalography (MEG; Cohen, 1968). The principle functions of particular frequency bands are therefore well established, with lower frequencies (delta, theta) observed during sleep or drowsiness, and higher frequencies (alpha, beta, gamma) associated with increasing levels of awareness and activity, whether excitatory or inhibitory. The amplitude and frequency of neuronal oscillations within a particular band can vary with the individual's state of alertness, the demands of the task and also between people; however, the source of this individual variability is not yet fully understood. Abnormalities in neuronal oscillations are often cited as markers of psychological or psychiatric disorders, yet it is clearly essential to understand the source and range of inter-individual variability within the healthy population before it is possible to determine the impact of differences in neuronal oscillations on patient populations.

This paper investigates individual variability in gamma (~30–100 Hz) oscillations in the visual cortex. Gamma oscillations have been associated with several functions in the brain, including basic sensory processing (Friedman-Hill et al. 2000; Edden et al. 2009; Donner & Siegel, 2011), movement generation (Cheyne et al. 2008), visual attention (Fries et al. 2001), short-term memory (Lisman & Idiart, 1995) and synchronisation of activity across the brain (Gray

& Singer, 1989; Singer, 1999; Maldonado et al. 2000). In the visual cortex, gamma activity measured in response to presentation of a stimulus consists of a high-amplitude, wide-frequency range 'spike' at stimulus onset followed by a lower amplitude and narrower frequency response that is present throughout the duration of the stimulus. The amplitude and frequency of this 'sustained' response is stable within participants across time, but varies between participants (Muthukumaraswamy et al. 2010), and this variability is likely to be behaviourally relevant: gamma amplitude correlates with task performance and perceptual experience (Hoogenboom et al. 2010; Rieder et al. 2011), while individual differences in the peak frequency of visual gamma oscillations correlate with behavioural measures of orientation discrimination (Edden et al. 2009). Importantly, a study of twins has revealed that the frequency of these narrow-band visual gamma oscillations is highly genetically determined (Van Pelt et al. 2012).

The neuronal mechanisms behind the production of gamma oscillations and the modulation of their frequency have been investigated both *in vivo* and through modelling of neurophysiological pathways. Gamma band neuronal activity may originate in 'chattering cells': pyramidal cells in superficial cortical layers, which have been said to fire repetitively at 20–70 Hz in response to depolarising currents (Gray & Mccormick, 1996). The synchronisation of this firing can be caused by the action of inhibitory or excitatory neurotransmitters, but is predominantly due to inhibition through gamma-aminobutyric acid-A (GABA$_A$) receptors (Bartos et al. 2007). The generation of gamma oscillations is therefore likely to be due to networks of GABA$_A$ interneurons modulating activity in pyramidal cells to give synchronous activity in the gamma frequency (Wang & Buzsáki, 1996). This activity produces rhythmic modulation of the membrane potential of pyramidal cells (Buzsaki & Chrobak, 1995), and this signal can be measured using EEG or MEG. The frequency of oscillations may depend on the strength of excitation, and on the balance between inhibitory and excitatory interactions between pyramidal cells and interneurons (Traub et al. 1996; Brunel & Wang, 2003), as well as on features of the visual stimulus such as movement (Friedman-Hill et al. 2000) or contrast (Ray & Maunsell, 2010).

Because GABA-ergic inhibition is important in the generation of gamma oscillations, individual differences in the concentration of GABA have been investigated in relation to gamma band activity. GABA concentration measured using magnetic resonance spectroscopy (MRS) has been shown to correlate positively with gamma frequency but not amplitude in visual (Edden et al. 2009; Muthukumaraswamy et al. 2009) and motor (Gaetz et al. 2011) cortices; however, this relationship was not replicated in a recent publication (Cousijn et al. 2014). The potential relationship between GABA concentration and gamma frequency might reflect a reduced excitation/inhibition ratio within the

network of pyramidal neurons and interneurons in participants with more GABA, which reduces the duration of a cycle of neuronal firing, inhibition then reactivation, leading to faster gamma oscillations in individuals with higher GABA concentration.

However, the relationship between gamma frequency and GABA concentration may be mediated by another factor that itself causes variability in both measures. For instance, the frequency of gamma oscillations in the visual cortex has also shown a positive correlation with retinotopically defined primary visual cortex (V1) and V2 surface area (Schwarzkopf et al. 2012). This finding was explained in terms of neurophysiological homogeneity, in that in a large V1, a smaller area of the visual field is represented by the same area of cortex as in a smaller V1, therefore homogeneity of factors such as neuronal stimulus preferences and receptor density is higher. In more homogenous areas, neurons oscillate at similar frequencies and conduction delays between neurons are shorter, therefore gamma oscillations are higher frequency. If the area of V1 is indeed predictive of gamma frequency, as there are more GABA$_A$ receptors in V1 than in other areas of the cortex (Zilles & Amunts, 2009), the correlation between gamma frequency and GABA concentration may be confounded by the area of V1 (Schwarzkopf et al. 2012).

Gamma-aminobutyric acid-ergic neurons and receptors are relatively evenly distributed in the horizontal plane in the cortex (Albus & Whale, 1994), but are more dense in certain layers of the cortex (layers II–III, IVA, IVC and VI; Hendry et al. 1990; Hendry & Huntsman, 1994; Munoz et al. 2001). If GABA-ergic neurons are involved in influencing the frequency of gamma oscillations, the thickness of V1 might also be expected to correlate with gamma frequency, because individuals with a thicker cortex may have more GABA in a given volume. A positive correlation between gamma frequency and cortical thickness has been reported in one previous study (Muthukumaraswamy et al. 2010), but not in others (Edden et al. 2009; Muthukumaraswamy et al. 2009; Schwarzkopf et al. 2012). A mediating factor in this relationship may also be the participants' age, as cortical thickness declines with age (Magnotta & Andreasen, 1999) and participant age has also shown an inverse relationship with gamma frequency in some (Muthukumaraswamy et al. 2010; Gaetz et al. 2011, 2012) but not all (Muthukumaraswamy et al. 2009; Schwarzkopf et al. 2012) studies. This inconsistency may be related to the small age ranges tested in the latter studies.

Various aspects of brain structure and composition have therefore been linked to individual differences in gamma frequency, but many of these variables are also correlated with each other. This shared variance makes discrimination of factors contributing to individual variability in gamma frequency more difficult. The small sample sizes often used in neuroimaging studies also limit the probability of detecting the true strength of correlations, given the noise

present in the measures. This study therefore aims to investigate multiple potential correlates of individual differences in gamma frequency in a larger sample of participants by bringing together multimodal neuroimaging data from several studies. The variables investigated are GABA concentration, V1 area and thickness, and age. Based on previous findings, it was hypothesised that GABA (Muthukumaraswamy et al. 2009) and V1 area (Schwarzkopf et al. 2012) would show the strongest relationships with gamma frequency.

Materials and methods

Participants

Participants were healthy volunteers with normal or corrected-to-normal vision, and all gave written informed consent. All procedures were approved by the local Ethics Committee. Data for the main analysis were collated from four studies: Muthukumaraswamy et al. (2009); Perry et al. (2013); S. Robson's PhD thesis; and previously unpublished data from G. McNamara and B. Davis. After removal of data from participants who were tested in more than one study or who did not show a clear gamma peak in visual cortex, there were 34 participants (33 male), mean age 29.4 years (SD 5.7). In an additional experimental analysis, pooled control data previously published by the current group (Shaw et al. 2013; Brealy et al. 2015) were used to validate relationships between age and gamma and V1 structure, as this dataset consisted of volunteers with a wider distribution of ages ($N = 25$; mean age = 33.7 years, SD = 11.9 years). These data could not be pooled with the main analysis as they use a slightly different gamma inducing visual paradigm.

Visual stimulation paradigm

In all studies, the paradigm consisted of presentation of a visual grating followed by a fixation-only baseline period. Participants made an index finger button press at stimulus offset. For the main experimental study, stimuli were 4 ° square patches containing vertical, stationary, maximum-contrast, three cycles per degree square wave gratings, and were presented on a mean luminance background. The top right corner of the grating was 0.5 ° below and to the left of the small red fixation point, except in two participants for whom the grating touched fixation (Perry et al. 2013). The duration of stimulus presentation was jittered between 1 and 2 s, with a 2–2.5 s baseline between stimuli, and there were between 70 and 200 trials depending on the study. For the second experimental study, the visual paradigm was similar except that stimuli were circularly windowed patches of diameter 4 ° and were presented with a jittered duration of 0.8–1.3 s. The paradigm was coded in Matlab (The Mathworks, Natick, MA, USA) and was presented on a Mitsubishi Diamond Pro 2070 monitor (1024 × 768 pixels, frame rate 100 Hz).

MEG acquisition and analysis

Magnetoencephalography data were obtained on a 275-channel CTF MEG system, with two channels switched off due to excessive sensor noise. An additional 29 reference channels were recorded for noise cancellation purposes, and the primary sensors were analysed as synthetic third-order gradiometers (Vrba & Robinson, 2001). Data

were sampled at 1200 Hz. The position of the head relative to the helmet was localised before and after the scan through three electromagnetic fiduciary coils placed at the nasion and left and right pre-auricular locations, to assess whether excessive head movement (> 5 mm) occurred during the scan.

Trials containing artefacts were discarded offline through manual inspection of the data. MEG data were co-registered with individuals' anatomical magnetic resonance imaging (MRI) scans using fiduciary markers placed at fixed distances from identifiable anatomical landmarks (nasion and tragus). A multiple local-spheres forward model (Huang et al. 1999) was derived for source localisation by fitting spheres to the brain surface extracted using FMRIB Software Library's Brain Extraction Tool (Smith, 2002). Estimates of the three-dimensional distribution of source power were derived for the whole head at 4 mm isotropic voxel resolution for each participant. Data were initially bandpass filtered using a fourth-order bi-directional IIR Butterworth filter in the 30–70 Hz range (40–60 Hz in 16 participants; Muthukumaraswamy et al. 2009). The synthetic aperture magnetometry (SAM) beamformer algorithm (Robinson & Vrba, 1999) was used to project extracranial field signals into source space, and images of the task-induced change in oscillatory power were derived from pseudo-T statistics of the contrast between source power in the stimulus and baseline phases (Robinson & Vrba, 1999; Vrba & Robinson, 2001; Hillebrand et al. 2005).

Locations of the peak amplitude in the gamma band in the visual cortex were identified for each participant from the pseudo-T statistic images. At these locations, a virtual sensor analysis was conducted whereby SAM beamformer weights were obtained from covariance matrices band-pass filtered between 30 and 70 Hz (0–100 Hz for 16 of the participants; Muthukumaraswamy et al. 2009). Data were then multiplied by the weights in order to produce a time-series of activity at that location for each trial and a time–frequency analysis was performed using the Hilbert transform. The signal was calculated as the percentage change in power relative to the average power at the gamma frequency in the baseline period. The peak frequency within the gamma range was then identified for each participant. Data were quality controlled by excluding participants who did not show a clear gamma peak.

MRS acquisition and analysis

Magnetic resonance data were acquired on a 3T GE HDx system (GE Healthcare, Chalfont St Giles, UK), with a body coil for transmission and an eight-channel receive-only head coil. MRS voxels were 3 × 3 × 3 cm and were positioned in the occipital cortex across the two hemispheres, with the lower edge aligned with the bottom of the occipital lobe, the anterior edge roughly aligned with the parieto-occipital sulcus and the posterior edge avoiding the scalp (Fig. 1a). GABA edited spectra were obtained using a MEGA-PRESS sequence (Mescher et al. 1998; Edden & Barker, 2007). The TE was 68 ms, TR was 1.8 s and Gaussian editing pulses were applied on alternate scans at 1.9 and 7.46 ppm. For 16 participants, there were two blocks of 512 acquisitions per voxel with a 20 ms editing pulse; for another 16 participants, one block of 512 acquisitions with a 16 ms editing pulse was obtained; while for two participants, two blocks of 332 acquisitions per voxel were acquired with a 16 ms editing pulse.

MRS data were analysed using the GABA Analysis Toolkit (Gannet: http://gabamrs.blogspot.co.uk/). A high-pass water filter was applied to produce a MEGA-PRESS difference spectrum. Automatic phasing of the GABA peaks was conducted, with small manual
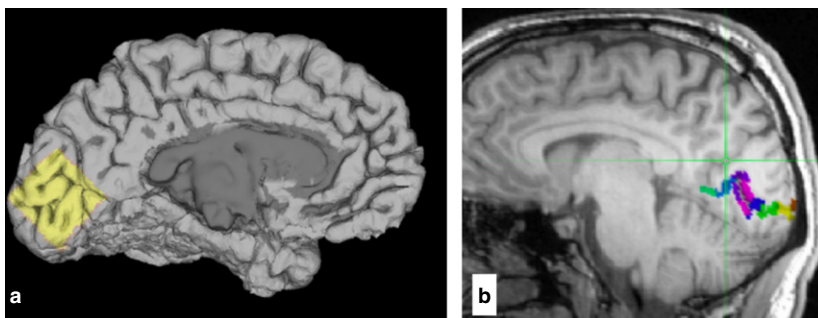
Fig. 1 MRS voxel position and anatomical V1 definition. (a) Position of MRS voxel in an example participant. (b) V1 area in an example participant, automatically defined using anatomical landmarks.

adjustments made where necessary. Because there are likely to be macromolecular contributions to the GABA signal in MRS, the measure is described as GABA+. The ratio of GABA+ to creatine was calculated, and the concentration of GABA+/Cr was converted to institutional units by accounting for the editing efficiency and the T1 and T2 relaxation times of the two molecules. Creatine was chosen as the reference molecule because it has been shown to be more repeatable than using water as the reference, or not using internal referencing (Bogner et al. 2010) and, in addition, the data were compared with a recent study on a large cohort of participants that demonstrated no relationship between gamma frequency and GABA+/Cr (Cousijn et al. 2014). In participants for whom two acquisitions were conducted, the mean GABA+/Cr concentration from these acquisitions was calculated.

V1 structure acquisition and analysis

Anatomical MRI scans of 1 mm isotropic resolution were acquired with a 3D Fast Spoiled Gradient-Echo sequence (TR/TE/inversion time = 7.8/3.0/450 ms; flip angle = 20 °). V1 was delineated in each individual's brain using an automated surface-based approach (Hinds et al. 2008), part of the *FreeSurfer* analysis package. In the first step of this analysis, the MRI is intensity corrected, skull-stripped and automatically segmented into grey matter, white matter and cerebrospinal fluid. This optimised and automated procedure is described in detail in a previous publication by the *FreeSurfer* developers (Dale et al. 1999). A 2D triangular mesh is then grown on the white matter to form an approximation of the pial grey matter surface for this individual. These mesh segmentations were inspected to ensure the correctness/integrity of the reconstructions. Each hemisphere is analysed separately. The grey matter surface is computationally inflated and transformed to a standard spherical geometry, in which the principal cortical folds, including the calcarine, are registered across individuals. This non-linear, spherical surface-based registration has been shown to provide an enhanced inter-subject registration of calcarine and peri-calcarine structures (Hinds et al. 2008, 2009), and therefore allows a probabilistic V1 atlas, defined in this spherical coordinate system, to be used to estimate the boundaries of V1 in each registered individual. Although it has been shown that the V1/V2 boundary does not have a simple relationship to the principal folds of the visual cortex (Zilles et al. 1997), the probabilistic method used here has been previously validated using direct comparison with V1 boundary estimates from post mortem *ex vivo* brains, high-resolution imagery of the stripe of Gennari, and functional retinotopic mapping in humans (Hinds et al. 2008, 2009). The algorithm results in a 2D triangular mesh representation of V1 for each individual, from which estimates of V1 area and V1 thickness can be directly estimated, separately for each hemisphere. Here, the relevant measures are for

the right hemisphere, as the grating was presented in the left visual field during the MEG experiments. Each V1 mesh was also segmented into 10 equal-length sections along the calcarine sulcus (Fig. 1b), and the area of the most posterior section of the right hemisphere of V1, corresponding to the representation of the foveal region of the visual field, was also obtained.

Results

Descriptive statistics for the measures of gamma frequency, GABA+ concentration and V1 thickness and area in the main dataset are shown in Table 1, and plots of the relationships between the key variables are shown in Fig. 2. All distributions were normal and there were no extreme outliers. Bivariate Pearson correlations indicated that gamma frequency showed a trend towards a significant positive correlation with GABA+/Cr concentration ($R = 0.34$, $P = 0.05$; Fig. 2e), while none of the correlations between gamma frequency and V1 thickness, RH V1 total area and RH V1 foveal area reached significance (all $R^2 < 0.078$, $P > 0.11$; Fig. 2b,d). All correlations are reported in Table S1, uncorrected for multiple comparisons.

Because the GABA+ value reported here is the ratio between the areas under the GABA and creatine peaks in the spectrum, it is possible (though physiologically less likely) that the correlation between gamma frequency and GABA+/Cr could be driven by a relationship with the creatine signal, rather than with GABA+. However, the correlation between gamma frequency and Cr/H_2O was small and non-significant ($R = -0.05$), suggesting that any relationship found between gamma frequency and GABA+ is most likely

Table 1 Mean and SD for variables measured.

	Mean (SD) for dataset 1	Mean (SD) for dataset 2
Age (years)	29.4 (5.7)	33.7 (11.9)
Gamma frequency (Hz)	52.5 (4.4)	44.8 (7.2)
GABA + concentration (IU)	1.40 (0.14)	Not available
Mean RH V1 thickness (mm)	1.84 (0.16)	1.85 (0.15)
Total RH V1 area (cm^2)	24.89 (3.5)	21.93 (3.85)
Foveal RH V1 area (cm^2)	1.32 (0.34)	Not available

GABA, gamma-aminobutyric acid.
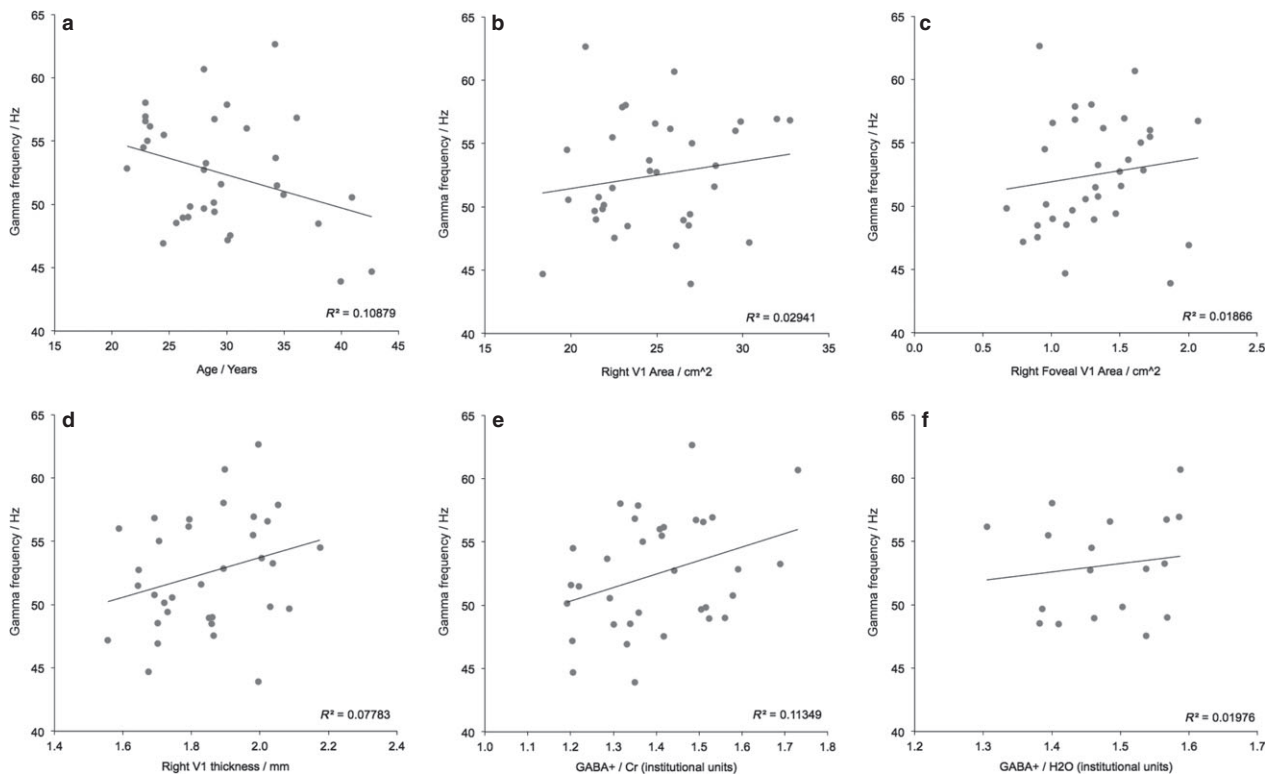
Fig. 2 Bivariate correlations for the first dataset. Correlations between individual peak gamma frequency and (a) age, (b) right V1 area, (c) foveal right V1 area, (d) right V1 thickness, (e) GABA+/Cr concentration and (f) GABA+/H_2O.

to be driven by GABA+ itself and hence should be unaffected by the choice of reference molecule.

Another potential factor in studies of visual gamma oscillations is age, which in these data showed trends towards significant inverse relationships with gamma frequency (Fig. 2a; $R = -0.33$, $P = 0.057$) and GABA+ ($R = -0.32$, $P = 0.065$), but not V1 area or thickness (all $R^2 < 0.066$, $P > 0.141$). Relationships with age are shown in Table S2. Additional partial correlations were therefore conducted using age as a covariate, which reduced the correlation between gamma frequency and GABA+ from $R = 0.34$ ($P = 0.05$) to $R = 0.26$ ($P = 0.15$). The correlations between gamma frequency and V1 structure were also all reduced by the addition of the covariate of age (all $R^2 < 0.045$, $P > 0.24$). These partial correlation results, reported in Table S1, suggest that age may be the dominant factor driving variance in visual gamma frequency, but that this relationship is not mediated via changes in V1 structure or variations in GABA+ concentration.

The correlation between age and gamma frequency has not been consistently reported across previous studies, and only approached significance in the main dataset here. This lack of consistency may be due to some studies using samples of volunteers of a similar age, reducing the opportunity to observe correlations across the full age range. Therefore this relationship was tested in a second dataset ($N = 25$) with a wider distribution of ages (mean = 33.7

years, SD = 11.9 years), but a statistically similar gamma frequency to the original dataset ($t_{60} = -1.928$, $P = 0.059$; box-plot shown in Fig. S1). As shown in Fig. 3a, age was highly inversely correlated with gamma frequency ($R = -0.69$, $P = 0.0001$), but there were no significant relationships between gamma frequency and right V1 thickness (Fig. 3b; $R^2 = 0.02$) or right V1 area (Fig. 3c; $R^2 = 0.001$) in this sample. In summary, as with the previous dataset, the only convincing dependency revealed in the data is that between gamma frequency and age.

The evidence for age-related changes in V1 structure in the two datasets combined were also examined ($N = 56$). These pooled relationships are depicted in Fig. 4, which reveals only weak dependencies on age for right V1 thickness ($R = -0.26$, $P = 0.14$) and area ($R = -0.24$, $P = 0.24$). In general, age only explained about 6–7% of the variance in area/thickness for the combined cohort. One reason for this perhaps lies in the large variance observed across the cohort at each age point. For example, at approximately age 20 years, Fig. 4(a) shows that V1 area varies from about 15 to 30 cm^2 in the current cohort. This large individual variability in V1 area has previously been shown in post mortem studies of the visual cortex (Andrews et al. 1997), in which the mean area of right V1 varied between 14.4 and 32.2 cm^2 (mean = 24.4 cm^2, SD = 4.9 cm^2). This variability is entirely consistent with the current estimates, determined non-invasively using structural MRI (mean = 23.5 cm^2, SD = 4.0 cm^2).
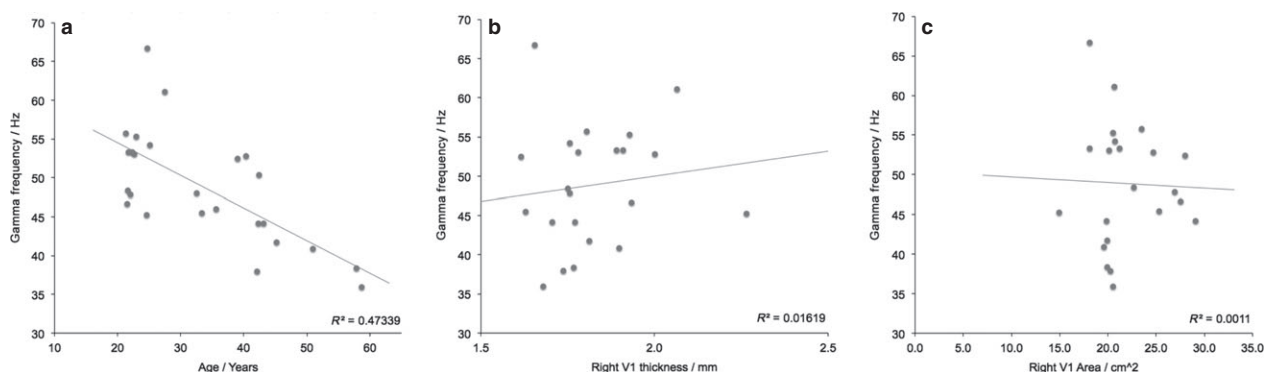
Fig. 3 Bivariate correlations for the second dataset. Correlations between individual peak gamma frequency and (a) age, (b) right V1 thickness and (c) right V1 area.
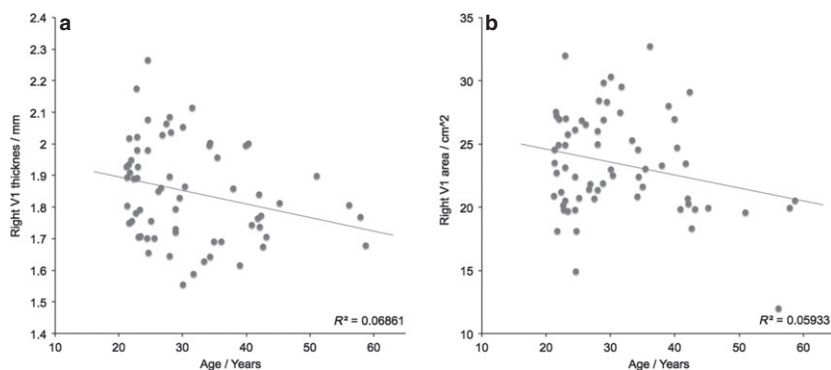
Fig. 4 The dependency of V1 structure on age for the two datasets combined. Both right V1 (a) thickness and (b) area only show a weak negative association with age.

It is therefore possible that ageing within an individual may be a strong modulator of both V1 thickness and age, but this is more difficult to reveal in a cross-sectional cohort because of large individual structural variability.

Discussion

The results of this study indicate that the relationship between individual differences in gamma frequency and GABA+ concentration may not be as strong as previously reported (Muthukumaraswamy et al. 2009), as only weak evidence of an association in an extended dataset was found here. There was also no significant correlation between the frequency of visual gamma oscillations and V1 structure (thickness or area), contrary to previous studies (Muthukumaraswamy et al. 2010; Schwarzkopf et al. 2012). Gamma frequency and GABA+ concentration showed a tendency to decrease with age and, in an independent dataset with a wider age range, age was strongly related to gamma frequency. Covarying for age reduced all correlations with gamma frequency, suggesting that age is an important mediating factor in the relationships between gamma frequency and V1 structure and GABA concentration, so should be taken into account – particularly in studies with a

wide age range of volunteers. Overall, this study does not definitively answer the question of which factors predict individual variability in visual gamma oscillations; it suggests that further variables may need to be explored, and that mediating factors might be involved, rather than a simple direct relationship between one brain feature and peak gamma frequency.

Previous reports of a correlation between individual differences in gamma frequency and GABA+ concentration (Edden et al. 2009; Muthukumaraswamy et al. 2009) were not replicated in a recent study using a large cohort of data (Cousijn et al. 2014). In the first dataset reported on here, there was a trend towards a correlation, but this may have been driven by inclusion of data from the original dataset from Muthukumaraswamy et al. (2009) as analysis of only the additional datasets did not show this relationship. In addition, the analyses presented here are not corrected for multiple comparisons so it is possible that the trend reported here is spurious. Although the correlation between GABA and gamma has been replicated in data from the motor cortex (Gaetz et al. 2011), small sample sizes have generally been used in such studies and spurious high correlations can occur by chance with small numbers of subjects. In any statistical analysis, the probability of

correctly detecting an effect increases with the sample size, the threshold chosen for significance and the true strength of the effect (Desmond & Glover, 2002). The significance threshold is typically set at 5%, but sample sizes in neuroimaging studies are often relatively small, so the power to detect effects is reduced. This issue will be conflated if the measurements are also noisy, because the repeatability of the analysis will be reduced. It is therefore important to use larger sample sizes and to ensure that the within-subject repeatability of measures is acceptable before meaningful correlations between measures can be made. MRS measures of GABA concentration (Bogner et al. 2010; Evans et al. 2010; Geramita et al. 2011; O'Gorman et al. 2011) and MEG measures of visual gamma oscillations (Muthukumaraswamy et al. 2010) are stable within individuals over time, so the repeatability of gamma and GABA seems to be acceptable; however, the impact of within-subject variability on the correlation between these two factors has not been empirically investigated and is likely to be greater than for each measure independently. Further work to investigate this issue would be beneficial.

This study also did not replicate previous findings of a correlation between gamma frequency and V1 area (Schwarzkopf et al. 2012). One potential explanation for this difference may be the use of different methods for delineating V1. In this study, V1 was identified anatomically based on the curvature of the gyri around the calcarine sulcus (Hinds et al. 2008), whereas Schwarzkopf and colleagues used retinotopic mapping. It is generally only possible to stimulate approximately 15 ° of the visual field in an MRI scanner due to the limited space in the bore in which to project images, so retinotopic mapping will not identify the whole of V1. It also requires good task compliance, so delineation of the boundaries of V1 may be more accurate in some participants than others. Similarly, with an anatomical method, the curvature of the gyri may be sharper in some individuals than others, allowing clearer definition of the boundaries of V1. These methods may therefore not provide the same rank order of participants in terms of the size of V1, which may explain the different relationships with gamma frequency reported in the two studies.

The current results suggest that age may be an important confound in measurements of individuals' gamma frequency. Although the correlation between age and gamma frequency only approached significance in the initial sample, this was likely due to the relatively narrow age range tested, as a strong correlation was observed in the sample with a wider age range. There is no mechanism by which age itself could directly affect gamma oscillation frequency, rather there must be an additional factor (such as an anatomical or physiological variable) that changes with age and that results in a decrease in gamma frequency. The relationship between gamma frequency and age is non-linear, beginning to decrease in adulthood (Gaetz et al. 2011), so is likely to reflect a feature of cortical maturation that occurs after neuronal growth and development has stabilised. The non-significant correlations of age with V1 structure observed in this study suggest that it may not be related to cell loss. In macaque monkeys, V1 cortical thickness does not change after adolescence, consistent with the current MR findings, but the percentage of neuropil gradually declines and, from puberty to older adulthood, synaptic density also decreases (Bourgeois & Rakic, 1993). The observed reduction in gamma frequency with age may therefore be driven by a reduction in synaptic connections that is not visible as a change in MR thickness estimates. However, in human adulthood, it has also been shown that there is little change in the number of neurons in the visual cortex (Leuba & Kraftsik, 1994) or the number of synapses across the brain (Bruer, 1999), therefore if true, the decrease in gamma frequency with age may not be related to a loss of neurons or synaptic connections. The strength of synaptic connections may be more relevant: synapses between pyramidal cells are strengthened by experience (Cheetham et al. 2012) so, perhaps in older participants, synaptic connections are sufficiently strong that they require less excitation to produce the same response and this reduced excitation decreases gamma frequency. Another potential mediator of the relationship between age and gamma frequency is contrast sensitivity: gamma frequency increases with contrast due to increased excitation of the cortex (Ray & Maunsell, 2010). Because contrast sensitivity to medium and high spatial frequencies decreases with age (Ross et al. 1985), visual gratings may induce less cortical excitation and consequently lower frequency gamma oscillations in older participants.

It is possible that age mediates the relationships between gamma frequency, GABA+ concentration and V1 structure by some independent mechanism. However, the correlations between gamma frequency and all of the variables in this study were quite small ($R^2 < 0.113$) even before controlling for the effect of age. This result suggests that there are other factors that contribute more to individual variability in gamma frequency than those investigated in this study. Further research could seek to identify these variables in order to gain a greater understanding of the source of variability in the frequency of gamma oscillations. For instance, computer modelling of cellular features of the cortex, such as the number of GABAergic interneurons or pyramidal cells, distances between synapses, or the density of $GABA_A$ receptors could help characterise factors influencing gamma frequency; or high-field MRS could be used to investigate whether the concentration of other neurotransmitters such as glutamate relate to gamma frequency. Another potential explanation for the low correlations between visual gamma oscillatory frequency and structural and chemical composition of the visual cortex is that the oscillations may be generated in a different area of the brain then transmitted to the visual cortex. Indeed, gamma can be present in long-range networks (Uhlhaas et al.

2009); however, further evidence in fact suggests that gamma is generated locally and reflects local processing, whereas lower frequency oscillations can originate in different regions and are more likely to be involved in longer distance communication (White et al. 2000; De Munck et al. 2007; Donner & Siegel, 2011). It is therefore unlikely that differences in location between the source and measurement of gamma oscillations explain the weak correlations observed here.

Concluding remarks

This exploratory study has shown that the source of individual differences in the frequency of visual gamma oscillations cannot yet be clearly identified. Of the variables investigated (GABA+ concentration, V1 area and V1 thickness), none showed strong correlations with gamma frequency; however, age was inversely correlated with gamma frequency and covarying for age reduced correlations with all other measures. Several other factors could play a role in modulating oscillatory frequency, such as features of tissue microstructure, other neurotransmitters, interactions with different brain regions and perhaps even genetics, therefore further investigation of these variables is required. It is likely that a number of factors, which may also covary with each other, combine to influence gamma frequency.

Acknowledgements

References

Albus K, Whale P (1994) The topography of tangential inhibitory connections in the postnatally developing and mature striate cortex of the cat. *Eur J Neurosci* **6**, 779–792.

Andrews TJ, Halpern SD, Purves D (1997) Correlated size variations in human visual cortex, lateral geniculate nucleus, and optic tract. *J Neurosci* **17**, 2859–2868.

Bartos M, Vida I, Jonas P (2007) Synaptic mechanisms of synchronized gamma oscillations in inhibitory interneuron networks. *Nat Rev Neurosci* **8**, 45–56.

Berger H (1929) Über das elektrenkephalogramm des menschen. *Archives für Psychiatrie* **87**, 527–570.

Bogner W, Gruber S, Doelken M, et al. (2010) *In vivo* quantification of intracerebral GABA by single-voxel (1)H-MRS – how reproducible are the results? *Eur J Radiol* **73**, 526–531.

Bourgeois JP, Rakic P (1993) Changes of synaptic density in the primary visual cortex of the macaque monkey from fetal to adult stage. *J Neurosci* **13**, 2801–2820.

Brealy JA, Shaw A, Richardson H, et al. (2015) Increased visual gamma power in schizoaffective bipolar disorder. *Psychol Med* **45**, 783–794.

Bruer J (1999) Neural connections: some you use, some you lose. *Phi Delta Kappan* **81**, 264–277.

Brunel N, Wang X-J (2003) What determines the frequency of fast network oscillations with irregular neural discharges? I. Synaptic dynamics and excitation-inhibition balance. *J Neurophysiol* **90**, 415–430.

Buzsaki G, Chrobak JJ (1995) Temporal structure in spatially organized neuronal ensembles: a role for interneuronal networks. *Curr Opin Neurobiol* **5**, 504–510.

Cheetham CEJ, Barnes SJ, Albieri G, et al. (2012) Pansynaptic enlargement at adult cortical connections strengthened by experience. *Cereb Cortex*, **24**, 521–531.

Cheyne D, Bells S, Ferrari P, et al. (2008) Self-paced movements induce high-frequency gamma oscillations in primary motor cortex. *NeuroImage* **42**, 332–342.

Cohen D (1968) Magnetoencephalography: evidence of magnetic fields produced by alpha-rhythm currents. *Science*, **161**, 784–786.

Cousijn H, Haegens S, Wallis G, et al. (2014) Resting GABA and glutamate concentrations do not predict visual gamma frequency or amplitude. *Proc Natl Acad Sci USA* **111**, 9301–9306.

Dale AM, Fischl B, Sereno MI (1999) Cortical surface-based analysis. I. Segmentation and surface reconstruction. *NeuroImage* **9**, 179–194.

De Munck JC, Gonçalves SI, Huijboom L, et al. (2007) The hemodynamic response of the alpha rhythm: an EEG/FMRI study. *NeuroImage* **35**, 1142–1151.

Desmond JE, Glover GH (2002) Estimating sample size in functional MRI (FMRI) neuroimaging studies: statistical power analyses. *J Neurosci Methods* **118**, 115–128.

Donner TH, Siegel M (2011) A framework for local cortical oscillation patterns. *Trends Cogn Sci*, **15**, 191–199.

Edden RAE, Barker P (2007) Spatial effects in the detection of aminobutyric acid: improved sensitivity at high fields using inner volume saturation. *Magn Reson Med* **58**, 1276–1282.

Edden RAE, Muthukumaraswamy SD, Freeman TCA, et al. (2009) Orientation discrimination performance is predicted by GABA concentration and gamma oscillation frequency in human primary visual cortex. *J Neurosci* **29**, 15 721–15 726.

Evans CJ, Mcgonigle DJ, Edden RAE (2010) Diurnal stability of gamma-aminobutyric acid concentration in visual and sensorimotor cortex. *J Magn Reson Imaging* **31**, 204–249.

Friedman-Hill S, Maldonado PE, Gray CM (2000) Dynamics of striate cortical activity in the alert macaque: I. Incidence and stimulus-dependence of gamma-band neuronal oscillations. *Cereb Cortex* **10**, 1105–1116.

Fries P, Reynolds JH, Rorie AE, et al. (2001) Modulation of oscillatory neuronal synchronization by selective visual attention. *Science* **291**, 1560–1563.

Gaetz W, Edgar JC, Wang DJ, et al. (2011) Relating MEG measured motor cortical oscillations to resting γ-aminobutyric acid (GABA) concentration. *NeuroImage* **55**, 616–621.

Gaetz W, Roberts TPL, Singh KD, et al. (2012) Functional and structural correlates of the aging brain: relating visual cortex (V1) gamma band responses to age-related structural change. *Hum Brain Mapp* **33**, 2035–2046.

Geramita M, Van Der Veen JW, Barnett AS, et al. (2011) Reproducibility of prefrontal γ-aminobutyric acid measurements with J-edited spectroscopy. *NMR Biomed* **24**, 1089–1098.

Gray C, Mccormick D (1996) Chattering cells: superficial pyramidal neurons contributing to the generation of synchronous oscillations in the visual cortex. *Science* **274**, 109–113.

Gray CM, Singer W (1989) Stimulus-specific neuronal oscillations in orientation columns of cat visual cortex. *Proc Natl Acad Sci USA* **86**, 1698–1702.

Hendry S, Huntsman M (1994) GABAA receptor subunit immunoreactivity in primate visual cortex: distribution in macaques and humans and regulation by visual input in adulthood. *J Neurosci* **14**, 2382–2401.

Hendry S, Fuchs J, Jones E (1990) Distribution and plasticity of immunocytochemically localized GABAA receptors in adult monkey visual cortex. *J Neurosci* **10**, 2439–2450.

Hillebrand A, Singh KD, Holliday IE, et al. (2005) A new approach to neuroimaging with magnetoencephalography. *Hum Brain Mapp* **25**, 199–211.

Hinds OP, Rajendran N, Polimeni JR, et al. (2008) Accurate prediction of V1 location from cortical folds in a surface coordinate system. *NeuroImage* **39**, 1585–1599.

Hinds O, Polimeni JR, Rajendran N, et al. (2009) Locating the functional and anatomical boundaries of human primary visual cortex. *NeuroImage* **46**(4), 915–922.

Hoogenboom N, Schoffelen J-M, Oostenveld R, et al. (2010) Visually induced gamma-band activity predicts speed of change detection in humans. *NeuroImage* **51**, 1162–1167.

Huang MX, Mosher JC, Leahy RM (1999) A sensor-weighted overlapping-sphere head model and exhaustive head model comparison for MEG. *Phys Med Biol* **44**, 423–440.

Leuba G, Kraftsik R (1994) Changes in volume, surface estimate, three-dimensional shape and total number of neurons of the human primary visual cortex from midgestation until old age. *Anat Embryol* **190**, 354–356.

Lisman J, Idiart M (1995) Storage of 7 ± 2 short-term memories in oscillatory subcycles. *Science* **267**, 1512–1515.

Magnotta V, Andreasen N (1999) Quantitative *in vivo* measurement of gyrification in the human brain: changes associated with aging. *Cereb Cortex* **9**, 151–160.

Maldonado P, Friedman-Hill S, Gray C (2000) Dynamics of striate cortical activity in the alert macaque: Ii. Fast time scale synchronization. *Cereb Cortex* **10**, 1117–1131.

Mescher M, Merkle H, Kirsch J, et al. (1998) Simultaneous *in vivo* spectral editing and water suppression. *NMR Biomed* **11**, 266–272.

Munoz A, Defelipe J, Jones EG (2001) Patterns of GABA(B)R1a, b receptor gene expression in monkey and human visual cortex. *Cereb Cortex* **11**, 104–113.

Muthukumaraswamy SD, Edden A, Jones D, et al. (2009) Resting GABA concentration predicts peak gamma frequency and FMRI amplitude in response to visual stimulation in humans. *Proc Natl Acad Sci USA* **106**, 2–7.

Muthukumaraswamy SD, Singh KD, Swettenham JB, et al. (2010) Visual gamma oscillations and evoked responses: variability, repeatability and structural MRI correlates. *NeuroImage* **49**, 3349–3357.

O'Gorman RL, Michels L, Edden RA, et al. (2011) *In vivo* detection of GABA and glutamate with MEGA-PRESS: reproducibility and gender effects. *J Magn Reson Imaging* **33**, 1262–1267.

Perry G, Hamandi K, Brindley LM, et al. (2013) The properties of induced gamma oscillations in human visual cortex show individual variability in their dependence on stimulus size. *NeuroImage*, **68**, 83–92.

Ray S, Maunsell JHR (2010) Differences in gamma frequencies across visual cortex restrict their possible use in computation. *Neuron* **67**, 885–896.

Rieder MK, Rahm BB, Williams JD, et al. (2011) Human gamma-band activity and behavior. *Int J Psychophysiol*, **79**, 39–48.

Robinson SE, Vrba J (1999) Functional neuroimaging by synthetic aperture magnetometry (SAM). In: *Recent Advances in Biomagnetism* . (eds Yoshimoto T, Kotani M, Kuriki S, Karibe H, Nakasato N), pp. 302–305. Sendai, Japan: Tohoku Univ. Press.

Ross JE, Clarke DD, Bron AJ (1985) Effect of age on contrast sensitivity function: uniocular and binocular findings. *Br J Ophthalmol* **69**, 51–56.

Schwarzkopf DS, Robertson DJ, Song C, et al. (2012) The frequency of visually induced γ-band oscillations depends on the size of early human visual cortex. *J Neurosci* **32**, 1507–1512.

Shaw A, Brealy J, Richardson H, et al. (2013) Marked reductions in visual evoked responses but not γ-aminobutyric acid concentrations or γ-band measures in remitted depression. *Biol Psychiatry* **73**, 691–698.

Singer W (1999) Neuronal synchrony: a versatile code for the definition of relations? *Neuron* **24**, 49–65.

Smith SM (2002) Fast robust automated brain extraction. *Hum Brain Mapp* **17**, 143–155.

Traub RD, Whittington MA, Colling SB, et al. (1996) Analysis of gamma rhythms in the rat hippocampus *in vitro* and *in vivo*. *J Physiol* **493**, 471–484.

Uhlhaas P, Pipa G, Lima B (2009) Neural synchrony in cortical networks: history, concept and current status. *Front Integr Neurosci* **3**, 1–19.

Van Pelt S, Boomsma DI, Fries P (2012) Magnetoencephalography in twins reveals a strong genetic determination of the peak frequency of visually induced γ-band synchronization. *J Neurosci* **32**, 3388–3392.

Vrba J, Robinson SE (2001) Signal processing in magnetoencephalography. *Methods* **25**, 249–271.

Wang XJ, Buzsáki G (1996) Gamma oscillation by synaptic inhibition in a hippocampal interneuronal network model. *J Neurosci* **16**, 6402–6413.

White JA, Banks MI, Pearce RA, et al. (2000) Networks of interneurons with fast and slow Υ-aminobutyric acid type a (GABAA) kinetics provide substrate for mixed gamma-theta rhythm. *Proc Natl Acad Sci USA* **97**, 8128–8133.

Zilles K, Amunts K (2009) Receptor mapping: architecture of the human cerebral cortex. *Curr Opin Neurol* **22**, 331–339.

Zilles K, Schleicher A, Langemann C, et al. (1997) Quantitative analysis of sulci in the human cerebral cortex: development, regional heterogeneity, gender difference, asymmetry, intersubject variability and cortical architecture. *Hum Brain Mapp* **5**, 218–221.

Supporting Information

Additional Supporting Information may be found in the online version of this article:

Table S1. All correlations between gamma frequency, GABA+, V1 thickness, total V1 area and foveal V1 area.
Table S2. Correlation of age with functional, chemical and structural features of V1.
Fig. S1. Boxplot of peak gamma frequency in the two datasets described.